

Supporting Information for “Airborne remote sensing of ocean wave directional wavenumber spectra in the marginal ice zone”

Peter Sutherland¹ and Jean-Claude Gascard²

¹Laboratoire d’Oceanographie Physique et Spatiale, L’Institut Francais de Recherche pour l’Exploitation de la Mer,
Plouzane, France.

²Laboratoire d’Océanographie et du Climat, Université Pierre et Marie Curie, Paris, France.

Contents

This supporting information contains the following:

1. Description of the technique used for estimating the ice fetch.
2. Plot of per-floe attenuation rate from Kohout and Meylan [2008].
3. Plot of the evolution of spectral parameters along the flight path.

1 Ice fetch

In this work, the complicated ice front meant that at any given location, \boldsymbol{x} , in the ice interior, waves travelling in different directions, θ , had travelled different distances through the ice.

The SAR imagery in supporting information figure 1.a shows a snapshot of ice cover taken at 2006/04/30 12:14 UTC. The green line in the figure indicates the ice edge, and was located using a manually tuned brightness threshold. The path through the ice over which the waves had travelled could then be found by starting from the flight segment location, and travelling in a reciprocal direction from the direction of wave propagation, until the open sea was reached.

The ice fetch, $X_{ice}(\boldsymbol{x}; \theta)$, is a directional function defined such that waves, at position \boldsymbol{x} , and travelling in direction θ , will have travelled a distance $X_{ice}(\boldsymbol{x}; \theta)$ through the ice from the open water. Supporting information figure 1.b shows a schematic of this calculation.

Corresponding author: Peter Sutherland, peter.sutherland@ifremer.fr

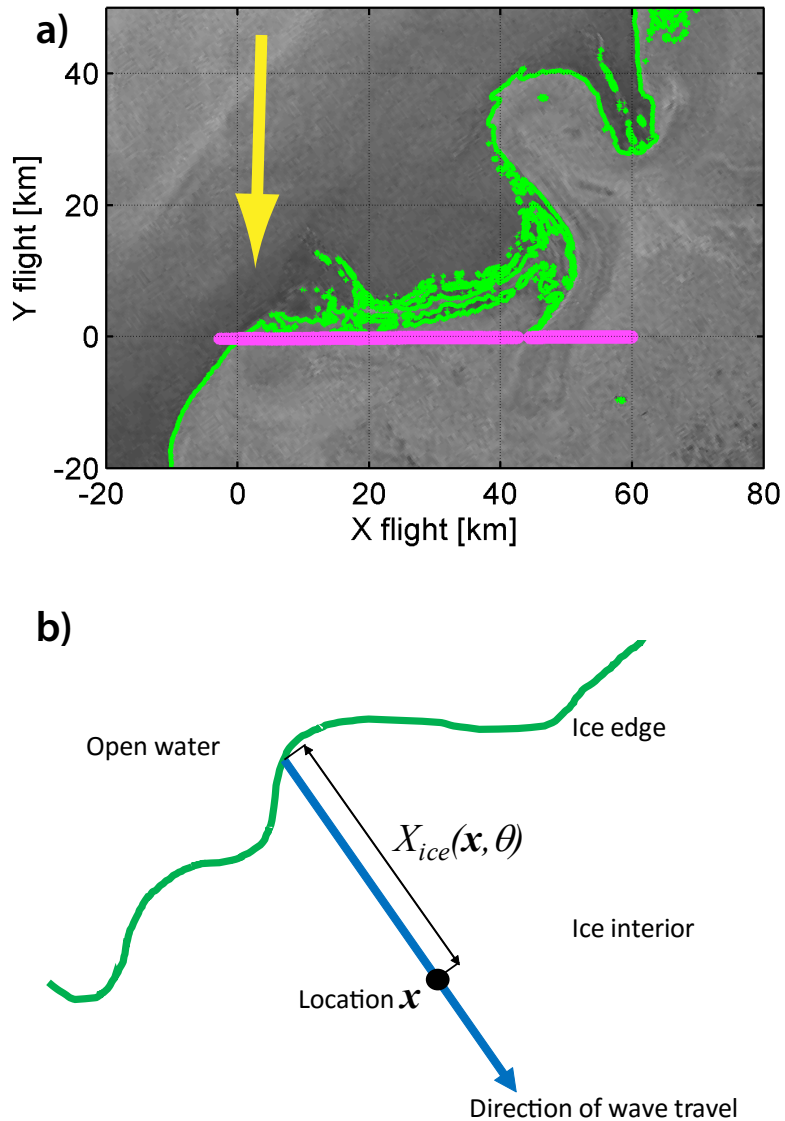


Figure 1: Estimation of ice fetch, X_{ice} . a) Research flight on 2006/04/30, relative to SAR imagery of sea ice. The gray background is wide-swath mode imagery from the ASAR instrument aboard ENVISAT, taken at 2006/04/30 12:14 UTC. The green line indicates the boundary between the open water and the MIZ. Sea ice is the generally lighter region on the right side of the image, open water is the darker region on the left. The pink line indicates the aircraft flight path. The aircraft flew in the negative x direction. b) Schematic of the definition of $X_{ice}(\mathbf{x}, \theta)$. Waves travel from the ice edge (green line) in direction θ (along the blue arrow) to location \mathbf{x} . The distance along the wave path from the ice edge to \mathbf{x} is $X_{ice}(\mathbf{x}, \theta)$.

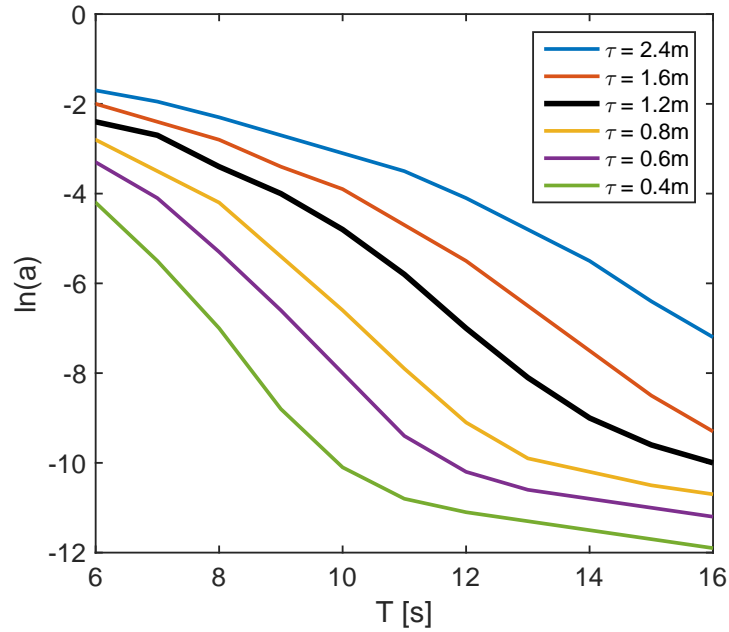


Figure 2: Reproduction of figure 6 from Kohout and Meylan [2008]. This shows the nondimensional per-floe attenuation rate, a , that was numerically calculated by Kohout and Meylan [2008] for their scattering-based wave attenuation model. Here, a is plotted as a function of wave period, T . Each line indicates a different ice floe thickness, τ . The curve used in this work, $\tau = 1.2\text{m}$, is the thick black line.

The ice fetch was calculated for each 4km segment of the flight path, with x set to the location of the centre of that flight segment.

2 Per-floe attenuation rate from Kohout and Meylan [2008]

See supporting information figure 2.

3 Evolution of spectral parameters along flight path

Supporting information figure 3 shows the spatial evolution of the spectral properties plotted in figure 4 of the main article.

Supporting information figure 3 also includes an additional model for the attenuation coefficient that was excluded from the main article due to space constraints. In it, attenuation is constant per wavelength. The attenuation coefficient then has a linear dependence on wavenum-

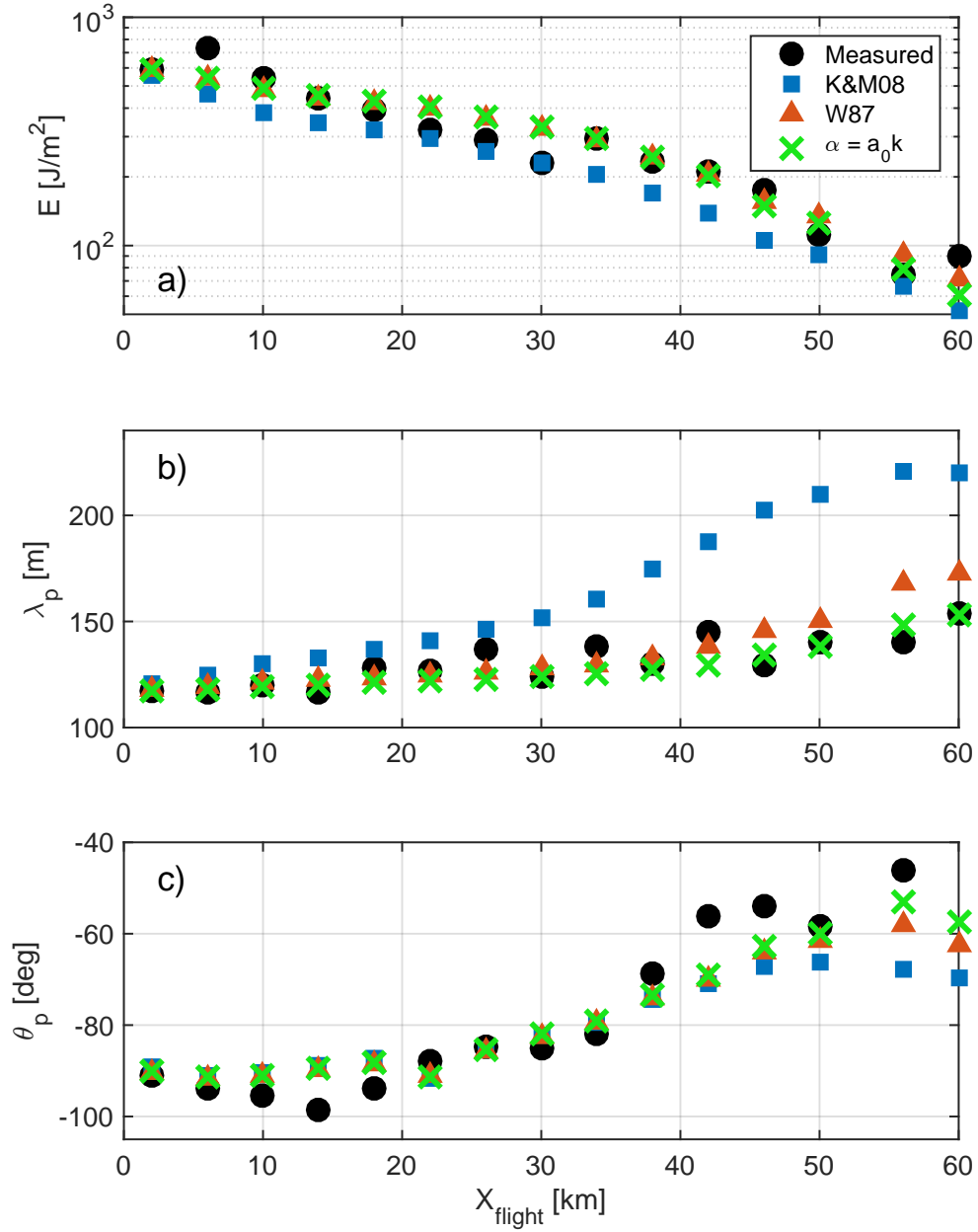


Figure 3: Evolution of spectral parameters along flight path. The black dots correspond to the measurements (the abscissæ in figure 4 in the paper, the blue squares correspond to the scattering model of [Kohout and Meylan, 2008], the red triangles correspond to the viscous fluid model of [Weber, 1987], and the green crosses correspond to the constant-dissipation-per-wavelength model. Each symbol represents an average over a 4 km section of flight path.

ber, and can be written as

$$\alpha(k) = a_0 k, \quad (1)$$

where a_0 is a nondimensional constant. Minimizing the least squares difference between the modelled and measured integrated energy, as in the viscous case above, gave $a_0 = 1.16 \times 10^{-3}$. The formulation in equation 1 bears some resemblance to that given in Meylan et al. [2014]. They observed the attenuation of waves with periods longer than approximately 10s, and found that wave field energy decayed with an attenuation coefficient of

$$\alpha(T) = \frac{c_1}{T^2} + \frac{c_2}{T^4}, \quad (2)$$

where T is the wave period. They fit their data with regression coefficients $c_1 = 2.12 \times 10^{-3} \text{s}^2/\text{m}$ and $c_2 = 4.59 \times 10^{-2} \text{s}^4/\text{m}$. Setting $c_2 = 0$, and then relating wave period to wavenumber using the linear deep water dispersion relation, $(2\pi/T)^2 = gk$, makes equations 1, and 2 equivalent, with $a_0 = c_1 g / (2\pi)^2$. In our work, the inclusion of the second term from equation 2 did not improve the fit to the data, and our a_0 was approximately 2.2 times the equivalent value observed by Meylan et al. [2014]. It is worth noting that this simple model matched the observed spectral parameters at least as well as the scattering and viscous layer models.

References

- Kohout, A. L., and M. H. Meylan, 2008: An elastic plate model for wave attenuation and ice floe breaking in the marginal ice zone. *Journal of Geophysical Research: Oceans*, **113** (C9), doi:10.1029/2007JC004434.
- Meylan, M. H., L. G. Bennetts, and A. L. Kohout, 2014: In situ measurements and analysis of ocean waves in the antarctic marginal ice zone. *Geophysical Research Letters*, **41** (14), 5046–5051, doi:10.1002/2014GL060809.
- Weber, J. E., 1987: Wave drift and wave attenuation in the marginal ice zone. *Journal of Physical Oceanography*, **17**, 2352–2361, doi:10.1175/1520-0485(1987)017<2351:WAAWDI>2.0.CO;2.